



Fabrication of Conductive Polymeric Films with Metallic Luster by Electroless Plating of Silver, Copper, and Nickel onto Polymethyl Methacrylate Beads

Ragia M. Mohsen, Yosreya M. Abu-Ayana, Samir M. M. Morsi*

National Research Centre, Polymer and Pigments Department, El Buhouth st., Dokki, Giza, 12622, Egypt



CrossMark

In Loving Memory of Late Professor Doctor "Mohamed Refaat Hussein Mahran"

Abstract

This study aims to synergize electrically conductive metals such as silver (Ag), copper (Cu), and nickel (Ni) with insulating plastics such as polymethyl methacrylate (PMMA), which has the advantages of lightweight, good mechanical properties, and reasonable prices. Ag, Cu, and Ni NPs are used to metalize micronized PMMA beads by first etching the surface with stannous chloride, then palladium chloride is used to create activate sites, and lastly electroless plating the metals is achieved by chemically reducing the precursor with hydrazine. FTIR, XRD, SEM, and EDX analyses have been used to demonstrate the metallization process. The metallized micronized beads were used to prepare films by both cold and hot compression molding at room temperature and 170°C respectively, using 100 lb/in² hydraulic pressure. The electrical conductivity of the molded films was evaluated. Both hot and cold molded Ag-metallized PMMA films showed outstanding conductivities in the range of 5×10^{-1} - 7×10^{-3} S/m. The electrical conductivity of Cu-metallized PMMA films was negatively affected by the accumulation of some formed copper oxides with the exception of hot molding 40% Cu which showed a conductivity of 1×10^{-1} S/m. For PMMA films metallized with 20-30% Ni and compressed by either cold or hot molding showed a conductivity of about 5×10^{-2} S/m. The metal plating process imparts the plastic films a high aesthetic appearance, prevents the accumulation of dust on them, facilitates their cleaning and. reveals good to excellent semiconductors that have many applications in electronic fields such as sensors.

Keywords: Metallization; electroless plating; metallic nanoparticles; polymethyl methacrylate.

1. Introduction

Polymers can typically sustain strong electric fields with limited conduction due to the large energy difference between the conduction band and the localized valence electron states, [1-3]. They are therefore regarded as insulators. However, some applications for polymers need to acquire them some electrical characteristics. Consequently, there has been a surge in research to build polymeric structures with electrical properties by fabricating composites with nano-metallic fillers [4-9]. Therefore, these polymeric nanocomposites can be used in many potential applications such as; photonics, medicine, drug delivery, biotechnology, electronics, pollution control, and environmental technology [2,3,10]. Even these nanocomposites can acquire superior antibacterial activity that may lead to biotechnological uses like biosensors and active ingredients in food packaging [11,12].

An important method for the synthesis of metal nanocomposites is by electroless deposition or coating of a uniform metal layer on the surface of the polymeric material [13-25]. This process is carried out through the chemical reduction of metal ions in an aqueous solution, and the subsequent precipitation of the metal without the use of electrical energy. In

general, electroless plating refers to an auto-catalytic process wherein only metal—typically utilized in plating metals like silver, copper, and nickel—is deposited on the surface. Silver is the most conductive metal, followed by copper, gold, and aluminum, but because of cost, copper is sometimes preferred.

The metallization process is considered a rapid progress in the electronic field due to its great advantages, as a simple and cost-effective alternative to conventional electroplating and its ability to deposit continuous and uniform metal layer onto non-conductive materials like plastics [24,25]. This leads to metal-polymer nanocomposites with low porosity and unique chemical, mechanical, electrical, and magnetic properties. Reducing agents such as sodium hypophosphite, formaldehyde, hydrazine, and borohydride are used in the reduction of metal ions to metals [3]. However, the electroless plating process itself is unstable, and its stability depends entirely on several factors including the substrate material, pre-treatment process, type of solution used, pH, and temperature during plating. Several techniques can be applied to improve the adhesion between plastics and metals, such as discharge treatment, chemical treatment, and flame treatment by activating the surface [26,27]. Traditional electroless plating of

*Corresponding author e-mail: samirmchemist@gmail.com.; (Samir M.M. Morsi).

Receive Date: 27 December 2023, **Revise Date:** 19 January 2024, **Accept Date:** 29 January 2024

DOI: 10.21608/ejchem.2024.258218.9101

©2024 National Information and Documentation Center (NIDOC)

polymer substrates involves pretreatment, activation, and deposition. The activation method is the key factor for subsequent successful electroless metal deposition. The activation route can be carried out either in a one-step method utilizing a colloidal mixture of SnCl_2 and PdCl_2 , or in a two-step method using a sensitizing solution of SnCl_2 followed by an activation solution of PdCl_2 [13,17]. Studies on percolation threshold in conductive polymer nanocomposites (CPNCs) is of such importance for scientists interested in CPNCs to determine the percolation threshold, which is the critical conductive filler concentration, where the composite turns abruptly from insulator to conductor as conductive pathways are formed [4, 28].

This study aimed to impart electrical characteristics to polymethyl methacrylate (PMMA) beads by depositing different concentrations of silver, nickel, and copper nanoparticles (NPs) using an electroless plating process. SnCl_2 and PdCl_2 were applied to the bead surfaces to set active sites for the metal deposition. Films of the metal-deposited PMMA beads were fabricated by cold and hot compression molding. Electrical studies were performed on these films to determine the electrical conductivity.

Materials and methods

2.1. Materials

The metal precursors are in the form of metal nitrate salts. Silver nitrate (AgNO_3), was obtained from Sisco Research Laboratories PVT. Ltd. India. Nickel nitrate hexahydrate ($\text{Ni}(\text{NO}_3)_2 \cdot 6\text{H}_2\text{O}$) and cupric nitrate trihydrate ($\text{Cu}(\text{NO}_3)_2 \cdot 3\text{H}_2\text{O}$) were both purchased from Alpha Chemika, India. Hydrazine monohydrate was supplied from Molekula Ltd, UK. Ethylene glycol (99.8%) as a stabilizing agent was obtained from SDFCL Fine Chemical Ltd. Methyl alcohol 99% was obtained from Sigma Chemicals. Sodium hydroxide pellets 99%, hydrochloric acid (35–38%) Sulfuric acid and were supplied from Fisher Scientific. Polymethyl methacrylate PMMA was obtained from IPsd SIGN Dentin Body. Potassium dichromate was obtained from Aldrich Chemicals Co. Ltd. Stannous chloride (SnCl_2) and palladium chloride (PdCl_2) $\geq 99.9\%$ were supplied from BDH Chemicals Ltd. England and Sigma-Aldrich, respectively.

2.2. Methodology

2.2.1. Electroless plating of Ag, Cu and Ni on PMMA beads

2.2.1.1. Pretreatment of PMMA beads:

30 gm of PMMA beads were ultrasonicated for 5-10 minutes in 80 ml 8% chromic acid solution (prepared from potassium dichromate and H_2SO_4).

The beads were rinsed well with deionized water to obtain an etched or roughened surface. The rinsed and etched beads were added to 50 ml stannous chloride solution (0.1 M SnCl_2 / 0.1 M HCl) and ultrasonicated for 40-60 minutes. The Sn^{2+} ions were adsorbed onto the surface of the beads by physical interactions with the polar ester groups. This is known as the sensitization step. Again, the beads were washed thoroughly with deionized water and filtered. The sensitized beads were then immersed into 50 ml acidified palladium chloride solution (1.4×10^{-3} M PdCl_2 / 0.25 M HCl) and stirred for 30 minutes. This is known as the activation step, where a redox reaction occurs on the surface of the sensitized beads in which Pd^{2+} oxidizes Sn^{2+} into Sn^{4+} and reduces to Pd^0 . As a consequence, tiny metallic Pd particles were generated on the surface of the PMMA beads which acted as catalytic sites. The activated beads were rinsed several times with deionized water and then filtered.

2.2.1.2. Electroless plating technique:

Electroless plating technique was used to metalize the surface of PMMA beads with Ag, Cu, and Ni nanoparticles (NPs). The pretreated beads were introduced into an electroless plating solution bath which was a salt solution of the metal ions in methanol at a ratio of 20 to 1 by weight of the metal salt. Metal nitrate was dissolved at different metal concentrations relative to PMMA (20, 30, and 40 weight %) to the PMMA beads. Hydrazine monohydrate was added to the solution at a ratio of 10 to 1 by weight of metal nitrate. The pH of the solution was adjusted to 8-9 by using NaOH. The reaction was carried out under reflux in the presence of ethylene glycol as a stabilizing agent at a concentration of 3.25-3.5%. A metal layer was deposited on the activated beads by the reduction of the metal ions (Ag^{+1} , Cu^{+2} , and Ni^{+2}) to metal atoms (Ag^0 , Cu^0 , and Ni^0). The metalized PMMA beads were filtered, thoroughly washed with distilled water, and dried at room temperature. The beads were labeled as PMAg, PMCu, and PMNi for Ag, Cu, and Ni -metalized PMMA beads, respectively. Also, the concentration of the metals to PMMA (20, 30, and 40) was added beside these symbols to specify the samples. For example; PMAg30 for Ag-metalized PMMA beads at a concentration of 30% silver to the beads.

2.2.2. Cold and hot compression molding of the metalized PMMA beads

Films of the metalized PMMA beads were fabricated by both cold (C) and hot (H) compression molding at room temperature and 170°C respectively, using 100 lb/in² hydraulic pressure. PMMA beads metalized with 20%, 30%, and 40% Ag, Cu, and Ni NPs were fabricated as films by cold molding at

room temperature. However, those beads plated with 20% and 30% were hot molded.

2.3. Characterization techniques

2.3.1. XRD patterns were obtained at room temperature using a Philips diffractometer (Model pw1390) employing Ni-filtered Cu K α radiation ($\lambda=1.5404\text{\AA}$), Japan, and operated at 40 kV and 40 mA in the 2θ range 5–80° at the scan speed of 0.05° per second. The diffraction angle, 2θ was scanned at a rate of 28/mi. Using Debye–Scherrer equation, the average particle size D was estimated [5]:

$$D = 0.9\lambda/(\beta \times \cos\theta)$$

Where: λ = X-ray wavelength (1.5404 Å), β = Line broadening and θ = The Bragg diffraction angle

2.3.2. Fourier transform infrared (FTIR) spectra were recorded by JASCO FTIR 6100 in the range of 4000–400 cm^{-1} with 4 cm^{-1} resolution and 50 scans with a scanning speed of 2 mm/s.

2.3.3. SEM micrographs were carried out by Quantum Field Emission Gun 250. Elemental identification and quantitative compositional information were provided by an energy-dispersive X-ray analyzer (EDX).

2.3.4. AC electrical conductivities were measured using Novocontrol GmbH Concept 40 broadband dielectric spectrometer (BDS).

Results & discussion

3.1. Metallization of PMMA beads with Ag, Cu, and Ni NPs

Figure 1 shows a schematic representation of the electroless plating process of Ag, Cu, and Ni metals on PMMA beads. Electroless plating is the method of depositing atomic active metals (such as silver, copper, nickel, gold, palladium, etc.) on a target surface without the use of electrical energy but rather a reducing chemical agent. The establishment of active sites on the PMMA surface is a crucial step in this process. To accomplish this, the method begins with using chromic acid to etch or roughen the surface of the beads. Sensitization by stannous ions (Sn^{+2}) comes next, where the ions interact physically with the polar groups of PMMA forming a uniform coat on the surface of the beads. Then, palladium ions (Pd^{+2}) oxidize Sn^{+2} to Sn^{+4} and are reduced to Pd^0 atoms to create the active sites. The treated PMMA beads are mixed with different metal salt solution, which serves as a precursor for Ag^{+1} , Cu^{+2} , and Ni^{+2} ions. The main process involves reducing the metal ions to metal atoms (Ag, Cu, and Ni) using hydrazine

as a reducing agent, thus depositing the metal atoms on the PMMA bead's active sites.

3.2. XRD analysis of metalized-PMMA beads

Figures 2 and 3 display the XRD patterns of the neat PMMA and the electroless-plated PMMA sample with Ag, Cu, and Ni NPs. The patterns were recorded in the angle range of 5 to 80°. Three broad peaks can be detected in pure PMMA (**Figure 2**) at $2\theta \sim 17.9^\circ$, 22.9° , and 41.3° indicating the amorphous structure of the polymer. When the metals are electroless-plated on the surface of PMMA, additional sharp peaks are formed indicating the crystalline structure of these metals. In addition to the broad peaks of PMMA, the Ag-metalized PMMA pattern (**Figure 3a**) shows four more distinct diffractions at 36.9° , 45.5° , 64.5° and 78.7° corresponding to (111), (200), (220), and (311) of the face-centered cubic silver crystalline planes, respectively, which is in accordance with JCPDS Silver File No. 04–0783 [29]. This signifies the development of crystalline silvery structures in the polymer matrix.

Also, the Cu-metalized PMMA XRD pattern (**Figure 3b**) shows two phases characterized by both crystalline and amorphous structures. The amorphous phase bound to PMMA which gave rise to broad diffractions at 2θ 17.8° and 22.6° . The high nanocrystalline property of the Cu NPs caused the strong and sharp peaks to lie at angles $2\theta = 41.1^\circ$, 49.8° , and 73.8° . These angles are related to the surface reflection of metallic Cu NPs planes (1 1 1), (2 0 0), and (2 2 0), respectively, which closely match with JCPDS File No. 4-836 [30]. The formation of CuO particles may be responsible for the occurrence of the minor peaks at 2θ values of 35.2° (0 0 2), 37.8° (2 0 0), 48.1° (-2 0 2), 53.1° (0 2 0), 57.8° (2 0 2), 61.1° (-1 1 3), and 66.6° (3 1 1) which are in good agreement to the mono-clinic phase (JCPDS Card, No. 48-1548) [31]. **Figure 3c**, XRD diffraction pattern of Ni-metalized PMMA, displays the produced crystalline nickel NPs besides the amorphous PMMA broad diffractions at $2\theta \approx 18.4^\circ$ and 22.7° . The three 2θ values at 44.8° , 52.2° , and 74.8° for planes (1 1 1), (2 0 0), and (2 2 0) are depicted to the face-centered cubic structure of Ni NPs (JCPDS card 01-078-07533).

The average particle size (D) of Ag, Cu, and Ni NPs can be calculated by Debye–Scherrer equation using the width of the (111) peaks. The calculated average sizes for the Ag, Cu, and Ni NPs in the metalized-PMMA were determined to be ~ 26 , 38, and 32, nm, respectively.

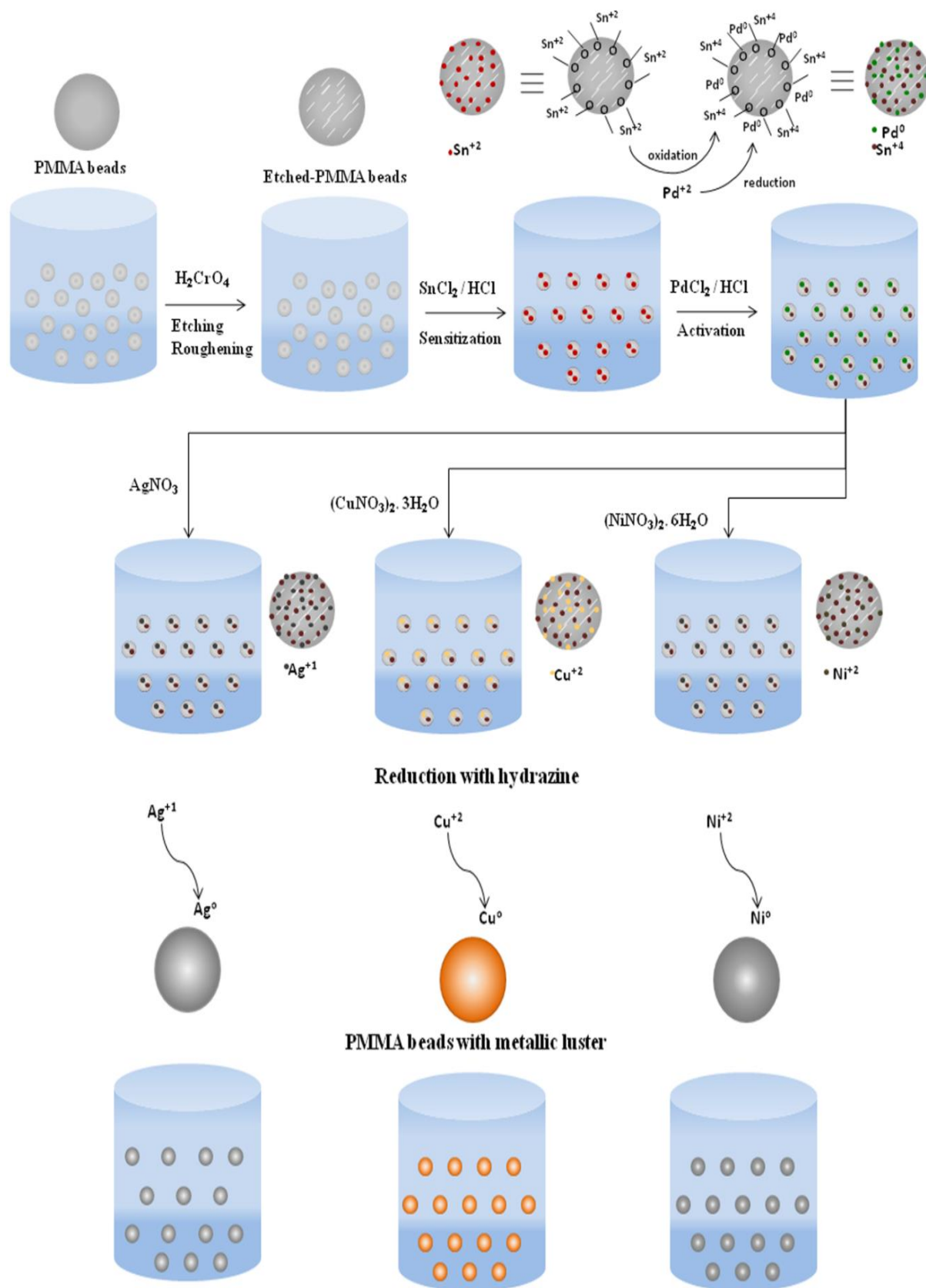


Fig. 1. Schematic presentation of the electroless metal plating onto PMMA beads.

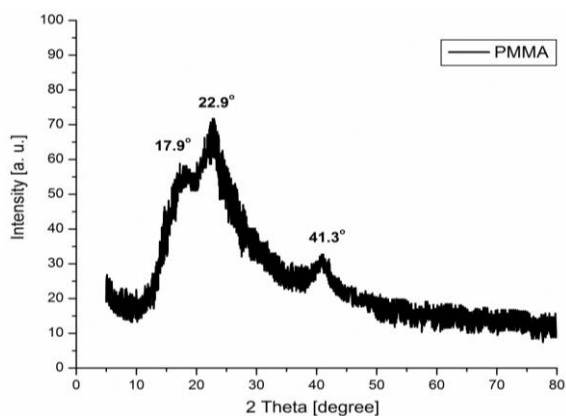


Fig. 2. XRD patterns of PMMA.

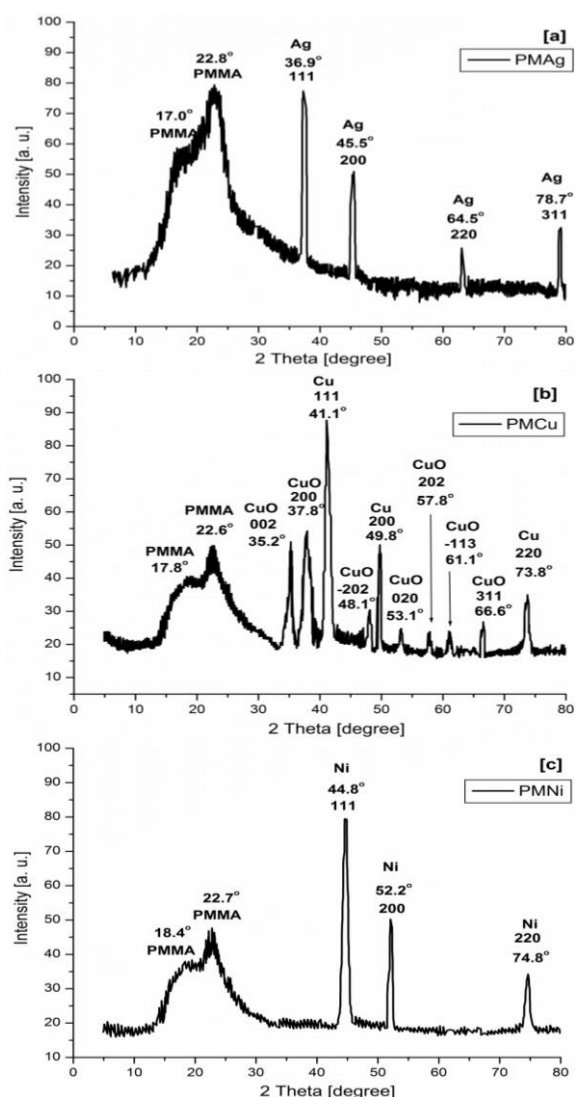


Fig. 3. XRD patterns of (a) PMAg, (b) PMCu, and (c) PMNi.

3.3. FTIR spectra of metalized-PMMA beads

Figure 4 shows the FTIR spectra of PMMA and the electroless-plated PMMA with Ag, Cu, and Ni NPs. The main peaks in the PMMA spectrum are those three peaks emanating from the

ester group at 1730 cm^{-1} (C=O stretch), 1190 cm^{-1} , and 1146 cm^{-1} (C-O stretch). This is in addition to C-H stretching and bending vibrations in the spectrum. For the metallized PMMA spectra, the C=O stretching vibration band shifted to higher wavenumbers (1766 cm^{-1} in PMAg, 1770 cm^{-1} in PMCu, 1773 cm^{-1} in PMNi) compared to the neat PMMA (1730 cm^{-1}). Also, higher shifts are obtained in C-O stretching bands, which is indicative of the interactions between the metal atoms and the ester groups in the polymer chain. The bands of metal can be observed at wavenumbers below 750 cm^{-1} .

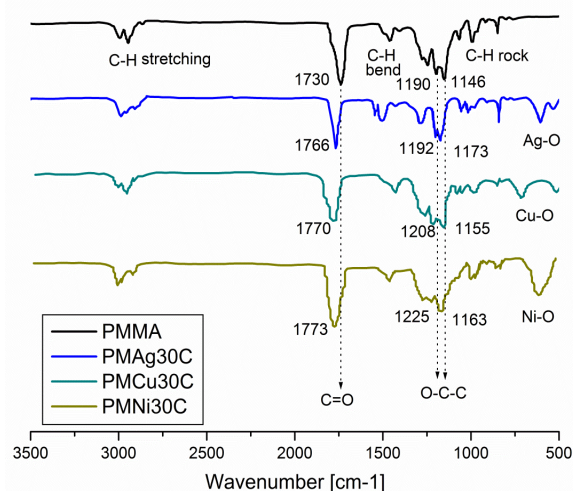


Fig. 4. FTIR Spectra of PMMA, PMAg, PMCu, and PMNi.

3.4. SEM and EDX analysis of metalized-PMMA beads

The SEM micrographs of the electroless plated PMMA beads with Ag, Cu, and Ni are displayed in Figure 5. The SEM image of PMAg (Figure 5a) demonstrates a compact and uniform silvery coat totally covering the PMMA beads. However, the SEM image of PMCu (Figure 5b) shows PMMA beads completely dispersed in the form of bunches of grapes, the size of which ranges between 300 and 500 nm, and are covered with copper metal. PMMA granules are distributed among the nickel NPs as beads in sporadic clusters (Figure 5c). These nickel-coated beads are about 500 nm in size.

Figure 6 shows the EDX analysis of the electroless-plated PMMA beads with Ag, Cu, and Ni. The success of the metallization process was evident in the spectra through the metal layers that completely dominate the surface of the beads. Only a silver signal was found by the EDX examination, indicating the success of the metallization process and that the resulting coating is chemically pure. On the other hand, the polymer's surface is covered by 86% copper in PMCu, and the oxygen atoms are dispersed more widely than in the other two

samples. These oxygen atoms can be attributed to both the PMMA itself and oxidized copper on the surface. These outcomes are consistent with the XRD results. However, 93% of nickel coats the surface of PMMA beads. Only 7% of the polymer atoms were detected in the EDX spectrum.

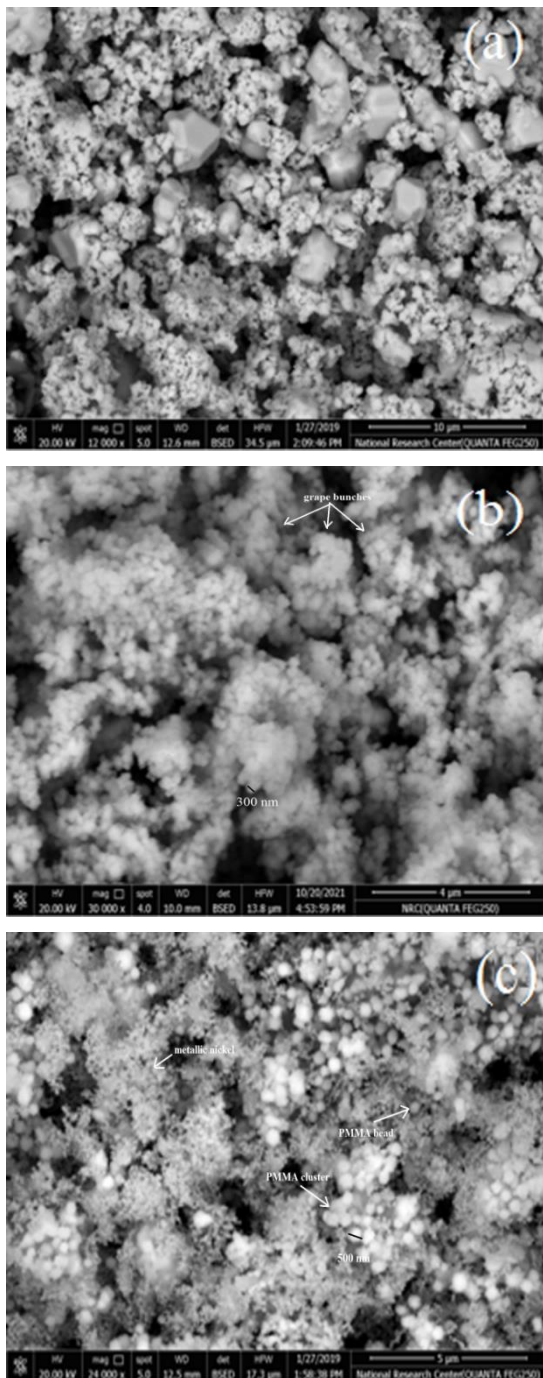


Fig. 5. SEM micrographs of PMAg (a), PMCu (b), and PMNi (c).

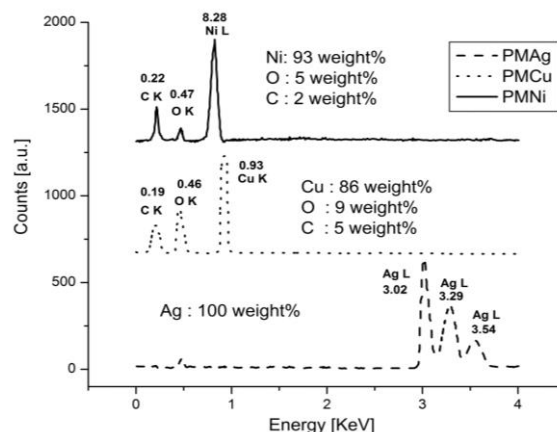


Fig. 6. EDX spectra of PMAg, PMCu, and PMNi.

3.5. Evaluation of AC electrical conductivity (σ_{ac}) of metal-coated PMMA films

The variation of AC conductivity (σ_{ac}) with frequency at room temperature of metalized films of PMMA with Ag, Cu, and Ni NPs fabricated by cold and hot compression molding techniques are shown in **Figures 7, 8, and 9**, respectively. The results revealed the following:

- The σ_{ac} of all metalized-PMMA with Ag films, either cold or hot molded, (**Figure 7**) is frequency independent of plateau type, which is considered as σ_{dc} conductivity.
- Films of cold compression molded PMMA metalized with Ag (**Figure 7**) show that as Ag conc. increases from 20% to 40%, the σ_{ac} decreases. This can be explained that silver nanoparticles having minute size can aggregate and separate from diffusivity as their concentration in the polymer matrix increases. The 20% Ag (PMAg20C) has σ_{dc} of 5×10^{-1} S/m, while 30% (PMAg30C) displayed σ_{dc} of 4×10^{-2} S/m.
- Films of hot compression molded PMMA metalized with Ag at 20% and 30% demonstrate that σ_{ac} increases with Ag conc. i.e., it behaves oppositely to cold molding, due to the heat of compression enhancing the diffusion of these particles within the matrix and thus increasing their electrical conductivity values. The 30% Ag conc. (PMAg30H) exhibited σ_{dc} of 1×10^{-1} S/m which was slightly higher than of the cold molded one at 30% (PMAg30C) 4×10^{-2} S/m. Therefore, PMAg20C and PMAg30H are the highest silver-metalized PMMA samples in terms of electrical conductivity.
- For Cu-metalized PMMA films (**Figure 8**), only 40% Cu film (PMCu40C) exhibited electrical conductivity, while the rest of the samples did not show the expected electrical results. This can be attributed to the formation

of a layer of non-conductive copper oxide, as shown in **Figure 3b** and **Figure 6**. However, the conductivity increases with the increase of frequency obeyed the empirical Jonscher universal law $\sigma ac \propto \omega^n$ where n is the frequency exponent [6]. The film (PMCu40C) exhibited a plateau-type behavior of conductivity with frequency and a σ_{dc} of 1×10^{-1} S/m.

- For cold compression molded Ni-metalized PMMA films (**Figure 9**), PMNi20C demonstrated no electrical conductivity at low frequency, but as the frequency increased, the conductivity increased, obeying the empirical Jonscher universal law [6]. As Ni NPs increased to 30%, a sudden increase in conductivity appeared with frequency that is of plateau-type behavior, followed by a sudden decrease at 40% Ni NPs $\approx 1 \times 10^{-10}$ S/m. Therefore, 30% Ni NPs film (PMNi30C) can be considered as the electrical percolation threshold conc. having σ_{dc} of 4×10^{-2} S/m.
- Hot compression molded Ni-metalized PMMA films, behave as Ag films (Fig.9), they exhibited higher electrical conductivities than cold compression molded samples. They revealed plateau behavior of conductivity with frequency variation. The 20-30% Ni NPs gave nearly the same σ_{dc} of 5×10^{-2} S/m.

From all the above results, the process of metallization of PMMA beads by metals was shown to be successful and the Ag-plated PMMA showed the highest electrical conductivity, which may be due to the completion of silver metallization on the surface of PMMA, as proven by EDX results (**Figure 6**).

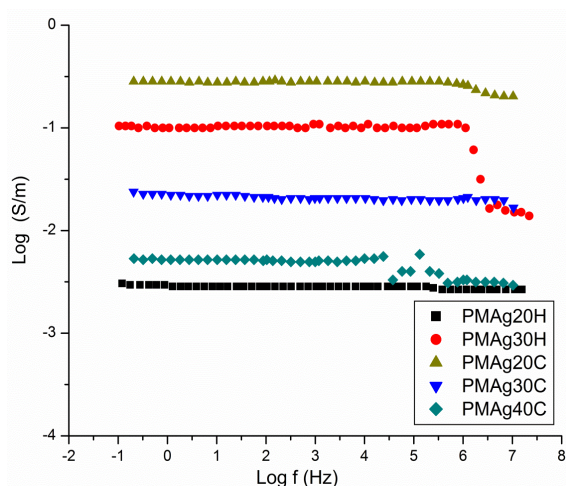


Fig. 7. Conductivity of Ag-metalized PMMA films.

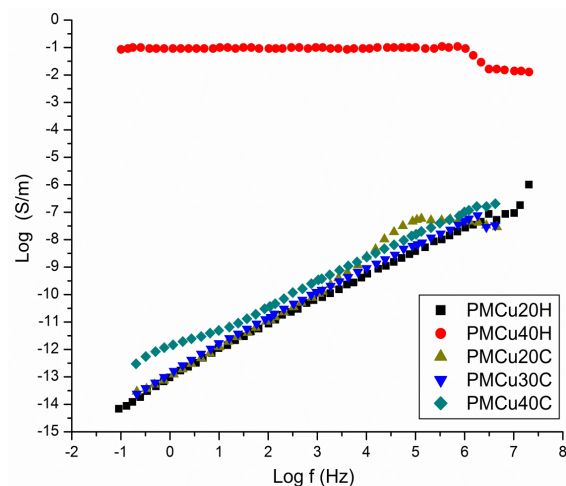


Fig. 8. Conductivity of Cu-metalized PMMA films.

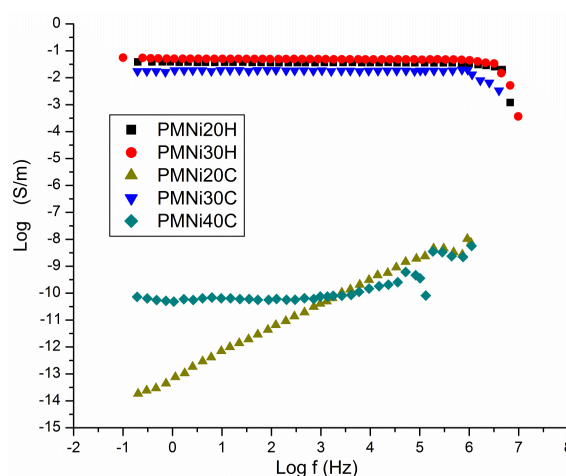


Fig. 9. Conductivity of Ni-metalized PMMA films.

Conclusions

Surface metallization of PMMA beads was performed using silver, copper, and nickel nanometals. The process was carried out by roughening the surface and then sensitizing it with stannous ions, followed by activating the surface through palladium atoms in a series of redox reactions. The process ended with the reduction of metal ions to deposit their atoms on the surface of the polymer beads. The metallization process has been proven through FTIR, XRD, and EDX analyses and SEM micrographs. X-ray spectra demonstrated the metallization process with the appearance of metal-specific peaks, especially 111 planes at 36.9° , 41.1° , and 44.8° for Ag, Cu, and Ni, respectively. It also showed the oxidation of copper atoms with the emergence of weak peaks characteristic to copper oxide. The SEM image of Ag-metalized PMMA revealed a compact and homogeneous silver coating covering the entire beads. In contrast, the SEM image of Cu-metalized PMMA depicted fully scattered beads in the shape of grape clusters that are 300–500 nm in size and

coated with copper metal. However, PMMA granules are spread in scattered clusters among the nickel NPs. EDX analysis also confirmed the complete deposition of silver on the surface of the Ag-metallized beads, while the oxidation of copper was proven by the spread of oxygen atoms on the surface of Cu-metallized PMMA. The electrical results showed that the conductivity decreased with the increase of silver particles for silver-metallized cold compression molded PMMA films. The opposite is true for hot compression molded specimens. These results can be considered from the perspective that silver nanoparticles having minute size are able to aggregate and separate from diffusivity as their concentration in the polymer matrix increases. However, the heat of compression enhanced the diffusion of these particles within the matrix and thus increased their electrical conductivity values. 20% cold-molded and 30% hot-molded Ag-metallized PMMA are considered the electrical percolation threshold conc., having σ_{dc} of 5×10^{-1} S/m, and 1×10^{-2} S/m, respectively. Only 40% copper-metallized compression molded PMMA film gave electrical conductivity (1×10^{-1} S/m), while the rest of the PMMA films did not show any conductivity due to the formation of a layer of copper oxide on them. Hot compression molded Ni-metallized PMMA films exhibited higher electrical conductivities than cold compression molded films revealing plateau-behavior of conductivity with frequency variation. The metallized PMMA films by 30% Ni NPs conc. using cold and hot compression molding gave σ_{dc} of 5×10^{-2} S/m. It can be concluded that electroless plating of PMMA with Ag showed the highest electrical conductivity due to the completion of silver metallization on the surface of PMMA, followed by Cu and Ni nanometals.

Conflicts of interest

The authors have no conflicts of interest to declare.

Acknowledgments

The authors greatly appreciate the National Research Center for the financial support of this research article derived from Project No. 110115.

References

- [1] A.K. Mishra, Conducting Polymers: Concepts and Applications, Journal of Atomic, Molecular, Condensate & Nano Physics, 5 (2018) 159–193.
- [2] S.K. ManirulHaque, J.A. Ardila-Rey, Y. Umar, A.A. Masud, F. Muhammad-Sukki, B.H. Jume, H. Rahman, N.A. Bani, Application and Suitability of Polymeric Materials as Insulators in Electrical Equipment, Energies, 14 (2021) 2758.
- [3] R.M. Mohsen, M.M. Selim, Y.M. Ayana, S.M.M. Morsi, A.M. Ghoneim, S.M. El-Sawy, Nanotechnology and nanomaterials, Chap. 7 in Nanomaterials & Nanotechnology, One Central Press (UK), (2016) 145-179.
- [4] Y.M. Abu-Ayana, R.M. Mohsen, A.A. Ghoneim, Synthesis and evaluation of semi-conductive polymer compositions, Polymer – Plastics Technology and Engineering, 45 (2006) 699-705.
- [5] R.M. Mohsen, S.M.M. Morsi, Y.M. Abu-ayana, A.M. Ghoneim, Synthesis of conductive Cu-core / Ag-subshell / polyaniline-shell nanocomposites and their antimicrobial activity, Egyptian Journal of Chemistry, 61 (2018) 939 – 952.
- [6] R.M. Mohsen, S.M.M. Morsi, M.M. Selim, A.M. Ghoneim, H.S. El-Sherif, Electrical, thermal, morphological and antibacterial studies of synthesized polyaniline/zinc oxide nanocomposites, Polymer Bulletin, 76 (2019) 1-21.
- [7] S.M.M. Morsi, H.S. Emira, S.M. El-Sawy, R.M. Mohsen, L.A. Khorshed, Synthesis and characterization of kaolinite / polyaniline nanocomposite and investigating their anticorrosive performance in chlorinated rubber/alkyd coatings, Polymer Composites, 40 (2019) 2777-2789.
- [8] S.M.M. Morsi, R. Mohsen, M. Selim, H. Elsherif, Sol-gel, hydrothermal, and combustion synthetic methods of zinc oxide nanoparticles and their modification with polyaniline for antimicrobial nanocomposites application, Egyptian Journal of Chemistry, 62 (2019) 1 – 24.
- [9] S.K. Mohamed, A.A. Abdou, A.S.A. Shalaby, R.M. Mohsen, A.A. Zikry, Synthesis and Characterization of Low Density Polyethylene Decorated with Ag/rGO Nanocomposite for Packaging Application, Egyptian Journal of Chemistry, 63 (2020) 1965 – 1976.
- [10] A.K. Mishra, Conducting Polymers: Concepts and Applications, Journal of Atomic, Molecular, Condensate & Nano Physics, 5 (2018) 159–193.
- [11] S.K. Manirul Haque, J.A. Ardila-Rey, Y. Umar, A.A. Masud, F. Muhammad-Sukki, B.H. Jume, H. Rahman, N.A. Bani, Application and Suitability of Polymeric Materials as Insulators in Electrical Equipment, Energies, 14 (2021) 2758.
- [12] A. Choudhury, Polyaniline / Silver nanocomposites: dielectric properties and ethanol vapor sensitivity, Sensors and Actuators, B chemical, 138 (2009) 318-325.
- [13] R.J. Rathsack, Electroless plating of plastics, U.S patent 3607350A (1967).
- [14] P.H. Wang, C.Y. Pan, Polymer metal composite microspheres: Preparation and characterization of poly(St-CO-AN)Ni microspheres, European Polymer Journal, 36 (2000) 2297-2300.
- [15] N. Bicak, S. Sungur, N. Tan, F. ben sebaa, Y. Deslandes, Metalization of polymer beads via polymer-supported hydrazines as reducing agents, Journal of Polymer Science Part A: Polymer Chemistry, 40 (2002) 748-754.

- [16] N.D. Sankir, R.O. Claus, An alternative method for selective metal deposition onto flexible materials, *Journal of Materials Processing Technology*, 196 (2008) 155-159.
- [17] M. Schlesinger, Electroless and electrodeposition of silver, *Modern Electroplating*, fifth Edition, M. Schlesinger Editor, Wiley & Sons, Inc. (2010).
- [18] M. Selvam, Electroless silver deposition on ABS plastic using CO (II) as reducing agent, *Transaction of the Institute of Metal Finishing*, 88 (2010) 198-203.
- [19] P. Dechasti, W. Trakarnpruk, ABS polymer by palladium and tin-free process, *Journal of Materials*, 21 (2011) 19-27.
- [20] S. Fujii, H. Hamasaki, H. Takeoka, T. Tsuruoka, K. Akamtsu, Y. Nakamura, Electroless nickel plating on polymer particles, *Journal of Colloid and Interface Science*, 430 (2014) 47-65.
- [21] F. Muench, Electroless Plating of Metal Nanomaterials, *ChemElectroChem*, 8 (2021) 2993-3012.
- [22] M. Mehdizadeh, M. Khorasani, S. Baghal, Direct electroplating of nickel on ABS plastic using polyaniline silver composite synthesized using different acids, *Journal of Coatings Technology and Research*, 15 (2018) 1433-1442.
- [23] P. Augustyn, A review on the direct electroplating of polymeric materials, *Journal of Materials Science*, 56 (2018) 14881-14899.
- [24] G.T.P. Azar, S. Danilova, L. Krishnan, Y. Fedutik, A.J. Cogley, Selective electroless copper plating of ink-jet printed textiles using a copper-silver, *Polymers (Basel)*, 14 (2022) 3467.
- [25] R. Muraliraja, R.A.S. Selvan, A. Selvakumar, M. Franco, T.R. Tamilarasan, U. Sanjith, W. Sha, J. Sudagar, A review of electroless coatings on non-metals: Bath conditions, properties and applications, *Journal of Alloys and Compounds*, 960 (2023) 170723.
- [26] Y. Deguchi, H. Yamagishi, S. Kirimura, Surface treatment of plastic material, U.S 4297187A (1981).
- [27] P. Huang, J. Hu, K. Wang, Y. Wang, The influence of etching time on the surface morphology of electroless nickel plated acrylic resins microspere, *Advanced Materials Research*, 1058 (2014) 89-92.
- [28] P.H.L. Coelho, M.S. Marchesin, A.R. Morales, J.R. Baraoli, Electrical percolation, morphological and dispersion properties of MWCNT/PMMA nanocomposites, *Material Research* 17 (2014) 127-132.
- [29] A.S. Lanje, S.J. Sharma, R.B. Pode, Synthesis of silver nanoparticles: a safer alternative to conventional antimicrobial and antibacterial agents, *J. Chem. Pharm. Res.* 2 (2010) 478.
- [30] T. Theivasanthi, M. Alagar, X-ray diffraction studies of copper nanopowder, *Arch. Phys. Res.* 1 (2010) 112-117.
- [31] M. Anbia, F. Aghadokht, Functionalization of silicon nanowires by iron oxide and copper for degradation of phenol, *Research on Chemical Intermediates*, 45 (2019) 1973-1984.